Status and Program of Concept Exploration Helical Mirror Device

A. V. Sudnikov[1,2], A. D. Beklemishev[1,2], V. V. Postupaev[1,2], I. A. Ivanov[1,2],
A. V. Burdakov[1,3], A. A. Inzhevatkina[2], N. A. Zhuravlev[2]

[1] *Budker Institute of Nuclear Physics, Novosibirsk, Russia*

[2] *Novosibirsk State University, Novosibirsk, Russia*

[3] *Novosibirsk State Technical University, Novosibirsk, Russia*

Introduction

Recent advances in magnetic mirrors demonstrated the quasistationary confinement of plasma with high relative pressure ($\beta \approx 60\%$) [1], mean energy of hot ions of 12 keV and the electron temperature up to 0.9 keV [2]. The mirror ratio in a simple open trap is limited by the achievable magnetic field and is supposed to be 15–20 in neutron source concepts [3]. Higher gain is possible with improved longitudinal confinement [4]. Existing method of multiple-mirror suppression of the axial flux combined with gas-dynamic central cell [5] can provide effective mirror ratios of the order of 100, which gives appropriate fusion gain for hybrids.

Recently, a new method of active plasma flow suppression in a helical magnetic field was proposed [6, 7]. That proposal renewed the idea of a plasma flow control with moving magnetic mirrors. Modulation of the guiding magnetic field travelling in the laboratory reference frame requires excessive energetics. Plasma rotation in $\boldsymbol{E}\times\boldsymbol{B}$ fields similar to vortex confinement [8] can be utilized to create periodical variations of helicoidal magnetic field moving upstream in plasma's frame of reference. These variations transfer momentum to trapped particles [9] and lead to plasma pumping towards the central trap. Theory predicts exponential dependence of the flow suppression on the magnetic structure length, that is more favorable then the power dependence in passive magnetic systems. Plasma biasing or natural ambipolar potential can drive the rotation. The first case also leads to plasma pinching [10]. Plasma acceleration can also be achieved [11]. Concept exploration device «SMOLA» with a helical mirror is being assembled now in BINP [7].

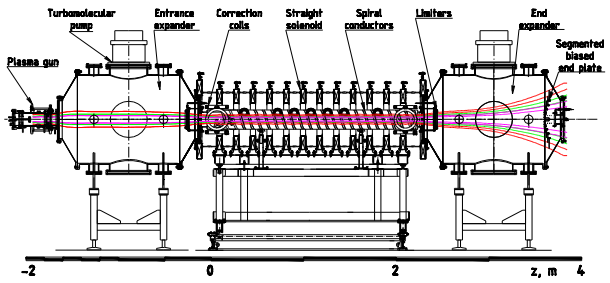

Fig. 1. SMOLA device. The plasma source, the vacuum vessel, the magnetic system and the biased limiters are shown. Magenta field line: edge of the cathode, green: edge of the anode, red: touching grounded vessel.

Plasma source operation

Plasma gun is based on the previously developed in Budker INP plasma source [12]. Typical plasma parameters for the prototype were $n \sim 2\times10^{19}$ m^{-3}, $T \sim 5$ eV. Ionization is performed by the electrons emitted from heated LaB_6 cathode [13]. Potentials of the anode and cathode are independent and magnetically insulated by the guide field 0.06–0.2 T of each other and of the grounded vacuum chamber. Plasma source is being tested now to find optimal plasma generation regimes.

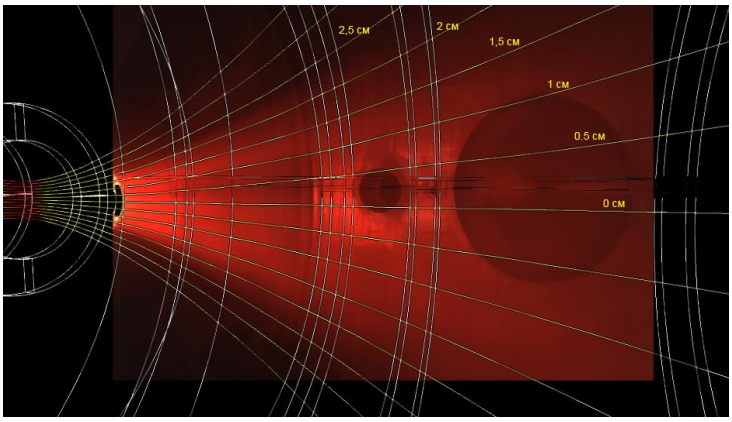

Fig. 2. Plasma stream in the expander. Magnetic coils and calculated field lines are shown. Numbers correspond to the starting radius of the field lines on the cathode.

Directed velocity at the plasma gun throat was measured by spatially resolved Doppler shift spectroscopy [14]. Spectrometer sightline was inclined at ~45° to the magnetic axis. In the axially symmetric case uniform shift of the spectral line corresponds to the exhaust velocity and its tilt is proportional to the angular rotation speed. For typical experiment these values are estimated as $V \sim 3\times10^6$ cm/s and $\omega \sim 10^6$ s^{-1}. The velocities stand in a good agreement with the estimations of the sound speed for $T_e \sim 5$ eV and radial electric field $E \sim 100$ V/cm.

In experiments discharge current $I = 210$ A was achieved (Fig. 5). Power delivered to the discharge determine the ionization rate, which can be estimated as $F \sim 2–3\times10^{21}$ ions/s during the flattop taking into account the cost of the ionization $E \sim 50$ eV/ion. At $V \sim 3\times10^6$ cm/s it corresponds to the plasma density $n \sim 1–2\times10^{19}$ m^{-3} in the plasma gun throat cross-section $S = 75$ cm^2. In the discussed experiments plasma was fueled with the continuous hydrogen flow of $F \sim 7\times10^{20}$ atoms/s starting at $t = 60$ ms. Discharge presumably fully ionizes incoming hydrogen and also recycles the gas neutralized on the end plates. Duration is limited by the energy

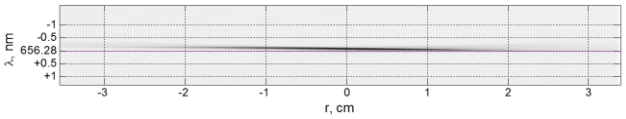

Fig. 3. Doppler shift corresponding to the plasma velocity. Magenta stands for the undisturbed spectral line

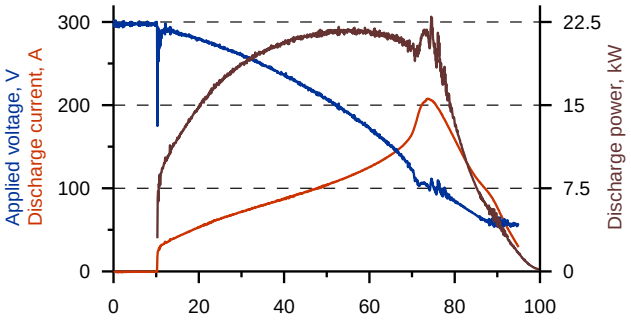

Fig. 4. Typical discharge current and applied voltage (left axis). Power delivered to the plasma (right axis).

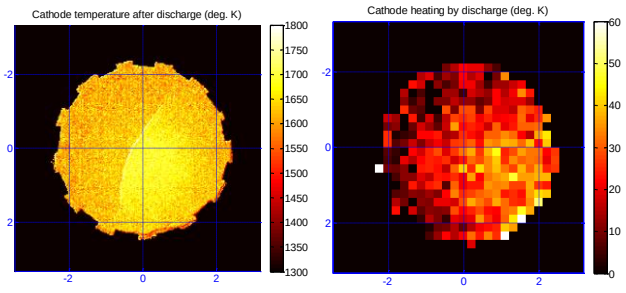

Fig. 5. Cathode temperature map and temperature rise in discharge

stored in the 1st stage of the discharge current source which is being upgraded at the moment of the presentation.

Discharge current heats the surface of the cathode thus improving emissivity. Temperature rise averaged over the cathode in typical shot is ~15 K (Fig. 6).

Required radial electric field estimations

Controlled profile of the radial electric field is induced inside the plasma by the individually controlled anode and cathode biases and radially segmented biased end-plate.

In the quasi-cylindrical geometry for hydrogen plasma, the dimensionless equation of continuity of plasma fluxes could be reduced to the following form [10]:

$$\frac{\partial}{\partial z} r\left(\frac{1}{\kappa\Lambda}\frac{\partial p}{\partial z}+(1+\kappa)n\zeta\frac{\partial \phi}{\partial r}\right)+\frac{\partial}{\partial r} r\left(\zeta\frac{\partial p}{\partial z}+D\frac{\partial n}{\partial r}\right)=0$$

Plasma density decays exponentially on any given field line. Flow suppression is also the function of the field line. In order to optimize the flow suppression over the plasma cross section, the radial electric field profile should change with radial distributions of the plasma density and field line inclination [10]. First estimations involves “solid-state” rotation with constant angular velocity. For this case radial electric field $E_r \sim r$. In hot plasma, diffusive term can be neglected. Characteristic length of plasma flow suppression for $n \sim \exp(-z/z_0)$ is:

$$z_0=\frac{1}{\Lambda\kappa\zeta}\left(\frac{1+\kappa}{1+T_i/T_e}\frac{\partial E_r}{\partial r}+\frac{\partial}{\partial r}\ln n_{z=0} r\zeta\right)^{-1}$$

In this case, suppression effectiveness drops significantly to the magnetic axis compared to the confinement in the peripheral region. This difference leads to the discharge contraction with distance. Narrow plasma stream on the axis should be suppressed in other ways.

In special case of equal flow suppression on any plasma radius, the radial electric field profile can be calculated (*this case definitely could not be achieved around the magnetic axis and may be not optimal in general*). Gaussian radial density profile was chosen as an estimate.

$$E_r=2\pi\frac{r}{a}\frac{1}{(1+\kappa)}\left(\frac{c_s}{V_{\phi,A}}\frac{a^2}{\kappa L z_0}+\frac{1}{\pi}\frac{a^2}{r_0^2}+4D_A\frac{z_0}{V_{\phi,A}r_0^2}\frac{L}{h}\left(\frac{r^2}{r_0^2}-1\right)\right)\frac{T}{ea}$$

$$\kappa\sim 1-\frac{1}{R(r)^2},\quad \kappa\underset{r\to 0}{\sim} r^2$$

At low magnetic fields (below 0.05 T) the required biasing voltage increases significantly. Moderate plasma parameters of SMOLA mirror (0.1–0.3 T, 10–100 eV) provide easily achievable estimations of the radial voltage $U \sim 200$ V.

Summary

A critical experiment should exclude all effects except for the helical confinement. It requires identical regimes of the plasma gun, the end-plates biasing and the magnetic field strength in the quasi-steady state. Magnetic fields of the opposite directions will cause different signs of the longitudinal force, thus changing the axial dependencies of the plasma density and velocity. Changes in the longitudinal plasma profile in different regimes will allow finding the scalings of the helical mirrors performance:

- varying plasma biasing at fixed solenoidal and helical magnetic fields;
- varying the helical component at fixed solenoidal field and biasing;
- varying the solenoidal component at fixed helical field and biasing;
- other experimental scalings (e.g., field strength, density, sort of gas, etc.).

Acknowledgements

This work was financially supported by Russian Science Foundation (project No. 14-50-00080). Parts of the study related to the modelling of the radial electric field distributions were supported by grant of President of Russian Federation SP-3356.2016.2.

[1] T.C. Simonen, et al., *J. Fusion Energy* **29**, 558 (2010)

[2] P.A. Bagryansky, et al., *Nuclear Fusion* **55**, 053009 (2015)

[3] A.V. Anikeev et al. *Materials* **8**, 8452 (2015)

[4] A. D. Beklemishev et al. *Fusion Sci. Technol.* **63 (No. 1T)**, 46 (2013)

[5] V.V. Postupaev, et al., Nuclear Fusion, 57, 036012 (2017).

[6] A. D. Beklemishev, *Fusion Sci. Technol*, **63 (No. 1T)**, 355 (2013).

[7] V.V. Postupaev et al., *Fusion Eng. Design,* **106**, 29 (May 2016).

[8] A.D. Beklemishev et al., *Fusion Sci. Technol*. **57**, 351 (2010):

[9] A. Burdakov et al., *Fusion Sci. Technol*. **51 (No. 2T)**, 106 (2007).

[10] A. D. Beklemishev, AIP Conference Proceedings. 1771, 040006 (2016).

[11] A.D. Beklemishev, *Phys. Plasmas*, **22, Iss.10**, 103506 (2015);

[12] T. Akhmetov et al., *Rev. sci. instr.*, **87**, 056106 (2016).

[13] V. I. Davydenko et al., *Plasma Phys. Reports*, **41, № 11**, 930 (2015).

[14] I. A. Ivanov et al., *Instruments and Experimental Techniques*, **59**, **№ 2**, 262 (2016).